GEOLOGICA CARPATHICA, FEBRUARY 2020, 71, 1, 73–82 https://doi.org/10.31577/GeolCarp.71.1.6

Monazite U–Th–total Pb age constraints on an early Permian volcanic event in the South Carpathians, Romania

ARTUR KĘDZIOR[1,✉], BARTOSZ BUDZYŃ[1], MIHAI EMILIAN POPA[2,3] and TOMASZ SIWECKI[1]

[1]Institute of Geological Sciences, Polish Academy of Sciences (ING PAN), Research Centre in Kraków, Senacka 1, PL–31002 Kraków, Poland; ✉ndkedzio@cyf-kr.edu.pl
[2]Southwest Petroleum University, School of Geosciences and Technology, 8 Xindu Ave., 610500 Xindu, Chengdu, China
[3]University of Bucharest, Faculty of Geology and Geophysics, Department of Geology and Doctoral School of Geology, Laboratory of Paleontology, 1 N. Bălcescu Ave., 010041 Bucharest, Romania

(Manuscript received July 1, 2019; accepted in revised form December 16, 2019)

Abstract: The sequence of Permian volcanic and volcaniclastic rocks (up to 2 km thick) in the Sirinia Basin (Svinița-Svinecea Mare sedimentary zone) of the Upper Danubian Units, South Carpathians, is considered to be the product of subaqueous volcanism passing into a subaerial volcanism and subsequent deposition by debris flow. The investigated volcano-sedimentary rocks are composed of a rhyolitic clastic framework embedded within a fine-grained matrix. The electron probe microanalyses of monazites in the rhyolite clasts and in the volcaniclastic matrix yielded a U–Th–total Pb mean age of 296±3.2 Ma. This result is the first to constrain the age of the volcanic activity event recorded in the volcaniclastic rocks of the Sirinia Basin. The monazite age also estimates the maximum depositional age of the volcano-sedimentary rocks as not older than early Permian (middle Asselian).

Keywords: Monazite, volcano-sedimentary rocks, South Carpathians, Romania.

Introduction

The Sirinia Basin, also known as the Svinița-Svinecea Mare sedimentary zone, is a sedimentary area belonging to the Upper Danubian Units of the South Carpathians, Romania (Codarcea et al. 1961; Năstăseanu et al. 1981; Berza et al. 1983, 1994). The basin represents the main cover of the Upper Danubian domain in the Almăj Mountains, bordered to the South by the Danube River, and to the North by the Bozovici Depression (Răileanu 1953, 1960). The basin occurs in the westernmost part of the Danubian Units which belong to the Alpine tectonic structure of the South Carpathians, overthrusted by the Supragetic, Getic and Severin Units (Munteanu-Murgoci 1905; Streckeisen 1934; Codarcea 1940; Codarcea et al. 1961; Năstăseanu et al. 1981, Berza et al. 1983, 1994; Pop et al. 1997). During the Permian, the Sirinia Basin recorded an extensional tectonic setting that resulted in generating a rhyolitic volcanic complex (Seghedi 2011).

This study focuses on the Buschmann area at the confluence of the Sirinia and Sirinca creeks in the central-southern part of the Sirinia Basin (Fig. 1). The Buschmann area is a part of the central syncline structure of the Sirinia Basin, which has a north–south oriented axis, with a normal eastern flank and a reversed western flank. In this area, the Buschmann coal mine extracting Lower Jurassic coals of the Cioaca Borii Formation was functional during the first half of the XXth century. The Permian formations occur towards the base of the sedimentary sequence, outcropping eastwards along the Sirinia creek around the former Stanca coal mine, at Buschmann, within the normal, eastern flank of the syncline and towards Cozilele and Stânei creeks, within its reversed, western flank. Along the Cozilele and Stânei creeks, former short, exploration galleries were dug during the second half of the XXth Century, searching for coals of the Carboniferous Cucuiova Formation (Stănoiu & Stan 1986). Despite the long-term research in this area, especially on the Jurassic sequences (Răileanu 1953, 1960; Pop et al. 1997), the knowledge about the substratum of these coal-bearing sequences remains limited. A modern study of the volcanic and volcaniclastic rocks was focused on their origin (Seghedi 2011), however, the age and relationship with older and younger strata remain uncertain.

This study aims to identify the age of volcaniclastic deposits exposed along the Danube valley and its tributaries. The analytical approach utilized the electron microprobe U–Th–total Pb dating of monazite. The obtained age data provide new insights into the regional interpretations with respect to the timing constraints of volcanic activity and estimated maximum depositional age of the volcaniclastic rocks in the Upper Danubian Units of the South Carpathians as well as in other parts of the Danubian Nappe System reported by Vozárová et al. (2009).

Geological background

The Sirinia Basin includes Paleozoic, Mesozoic and Cenozoic sediments, unconformably overlying the crystalline basement represented by the Ielova or Mraconia metamorphic units (Răileanu 1953; Năstăseanu et al. 1981; Berza et al.

1994). The Paleozoic cycle includes Upper Carboniferous and Permian formations, the Mesozoic cycle includes Lower Jurassic to Upper Cretaceous formations, while the Cenozoic includes mainly Miocene sequences (Răileanu 1953, 1960; Răileanu et al. 1963; Petrescu et al. 1987; Preda et al. 1994; Popa & Anastasiu 2019). The following two formations related to the Paleozoic cycle are distinguished (Fig. 1):

1. The Cucuiova Formation (Stănoiu & Stan 1986) is a terrestrial, coal bearing formation represented by sandstones, conglomerates, mudstones, coal seams and trachyte flows; with the latter occurring towards the top of the formation (Răileanu 1953; Răileanu et al. 1963; Năstăseanu et al. 1973; Dragastan et al. 1997; Popa 2005; Popa & Cleal 2012). The formation is 150–300 m thick, with strong lateral variations in thickness and facies. The occurrence of seed-ferns and of other floral remains from Baia Nouă coal mine identify the age of the Cucuiova Formation as Westphalian A – Stephanian (Popa & Cleal 2012).

2. The Trescovăț Formation (Stănoiu & Stan 1986), Early Permian in age, is also a volcanogenic–terrestrial formation unconformably overlying the Cucuiova Formation, represented by mudstones, sandstones (especially by red beds), conglomerates, lacustrine limestone lenses, rhyolites and volcaniclastics (Răileanu 1953, 1960; Năstăseanu et al. 1973; Seghedi et al. 2001; Seghedi 2011). We consider that separating two formations as the Povalina and the Trescovăț

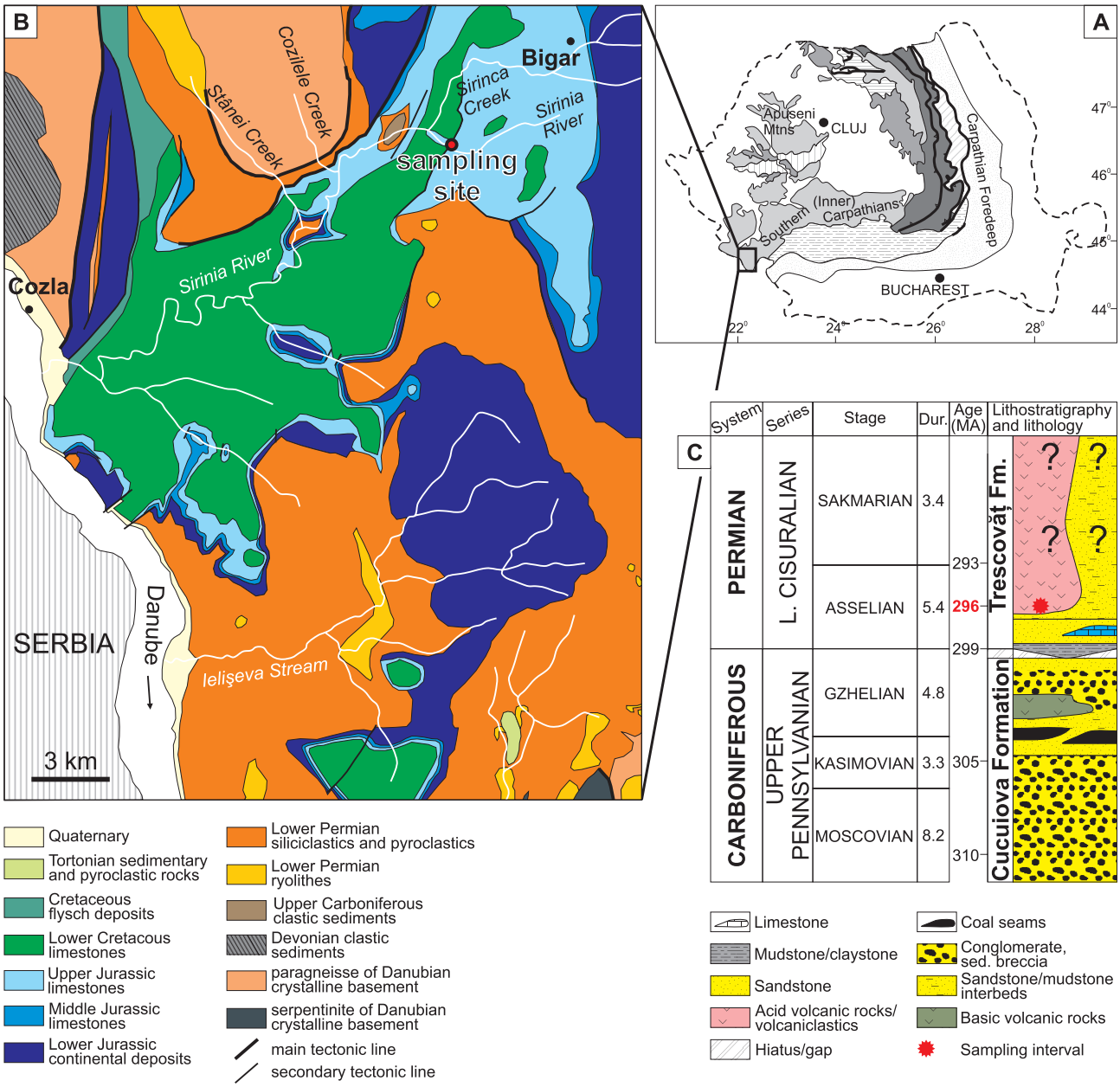

Fig. 1. Geological map of the Sirinia Basin after Răileanu (1960) (**B**), as part of the geological structure of the South Carpathians (**A**) with lithostratigraphy of the Permo–Carboniferous strata according to Vozárová et al. (2009) and Seghedi et al. (2001) (**C**).

formations of Stănoiu & Stan (1986) is irrelevant, because of the continuous sequence of red beds, rhyolites and volcanoclastics, therefore the former Povalina Formation of Stănoiu & Stan (1986) should not be used as a separate stratigraphic unit.

The Lower Jurassic to Upper Cretaceous marine deposits unconformably overlie both the post-Variscan sequences and the crystalline basement.

The early subaqueous domes (isolated or as clusters) composed of massive lava pass laterally into subhorizontal cm–mm-size fluidal textures and to autoclastic breccias. The breccias are massive to incipiently stratified and are constituted of angular glassy unsorted rhyolitic fragments of metre–decimetre-size decreasing laterally to cm-size, in a fine-grained matrix of the same composition (Seghedi 2011). The Sirinia Valley is strongly tectonized and the outcrops with volcaniclastic deposits of the Sirinia Syncline are very small in the Buschmann area, giving no insight into the wider geological context of this occurrence.

The Permian succession of the Trescovăț Formation of the Sirinia Basin has been considered to record a surtseyan sequence, from underwater, lacustrine eruptions to sub-aerial eruptions which were finally reworked in a fluviatile system to the top of the Permian Trescovăț Formation, during the Early Permian (Seghedi 2011). The following volcanic phases were identified (Seghedi 2011): (i) the subaqueous eruption phase; (ii) the subaqueous-subaerial explosive phase; (iii) the emergent effusive phase; (iv) the erosional, post-volcanic stage.

The volcaniclastic rocks from the Sirinia Basin, which are the main subject of the current study, represent hyaloclastic breccia made of unsorted angular rhyolitic fragments up to 7 cm in diameter with finer matrix as well as subaerial and Surtseyan pyroclastic deposits and associated rocks. The composition of the phenocrysts (plagioclase — 5–12 %; quartz — 5–8 %; amphibole — 3–4 %; and biotite — 1–3 %) and microgranular groundmass (about 80–65 %) has the same mineral content (Seghedi 2011). The rocks are variably carbonatized, chloritized or silicified. The SiO_2 contents of all the volcanic deposits in the Sirinia Basin vary between 74–80 % (Stan et al. 1986).

Samples and analytical methods

The samples have been collected from an outcrop of the Trescovăț Formation rocks, close to the Buschmann mine, on the left bank of the Sirinia valley, (GPS coordinates 44.636547°N, 22.088252°E). The preliminary observations in thin sections and the sample selection for monazite dating were performed using a Hitachi S-4700 field emission scanning electron microscope equipped with an energy dispersive spectrometer (EDS) at the Institute of Geological Sciences, Jagiellonian University (Kraków, Poland).

The compositional analyses of monazite for U–Th–total Pb dating were performed using a Cameca SX 100 electron microprobe at the Department of Electron Microanalysis, State Geological Institute of Dionýz Štúr (Bratislava, Slovak Republic). The monazite was analysed using a 15 kV accelerating voltage, 180 nA beam current, and 3 µm beam size focused on a carbon coated thin section. Depending on the crystal size, from 1 to 12 analyses were performed on each monazite. The chemical compositions of monazite were recalculated using age equations from Montel et al. (1996) and evaluated using in-house software to plot histograms and isochrones (P. Konečný, unpublished). For more analytical details see Konečný et al. (2018). The ISOPLOT v. 4.16 (Ludwig 2012) has been used to plot weighted average plots and to calculate mean ages. The BSE images and compositional WDS X-ray maps were collected using JEOL SuperProbe JXA-8230 Electron Probe Microanalyser (EPMA) at the Laboratory of Critical Elements AGH-KGHM, AGH-University of Science and Technology, Kraków, Poland.

Results

Sample description

The volcanic breccia contains rounded rhyolitic clasts with sizes up to several cm (Fig. 2). The rhyolitic clasts contain anhedral to subhedral crystals of quartz and twinned plagioclase dispersed in very-fine grained, clay groundmass (Fig. 3G–H). The quartz phenocrysts occasionally preserve crystal faces. The feldspars are partially to completely altered. Rare biotite flakes are partially chloritized. Carbonate grains

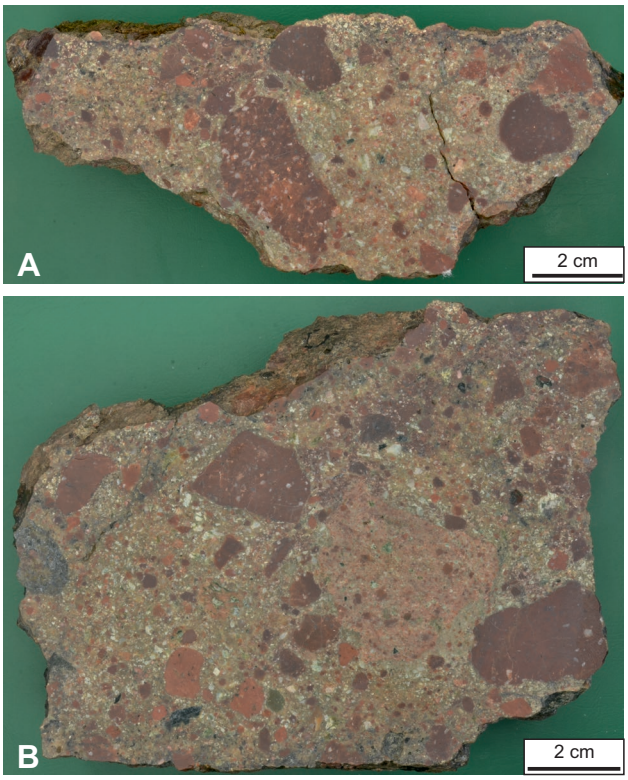

Fig. 2. Volcaniclastic breccia containing analysed monazite crystals**.** Samples RU04B (**A**) and RU04C (**B**).

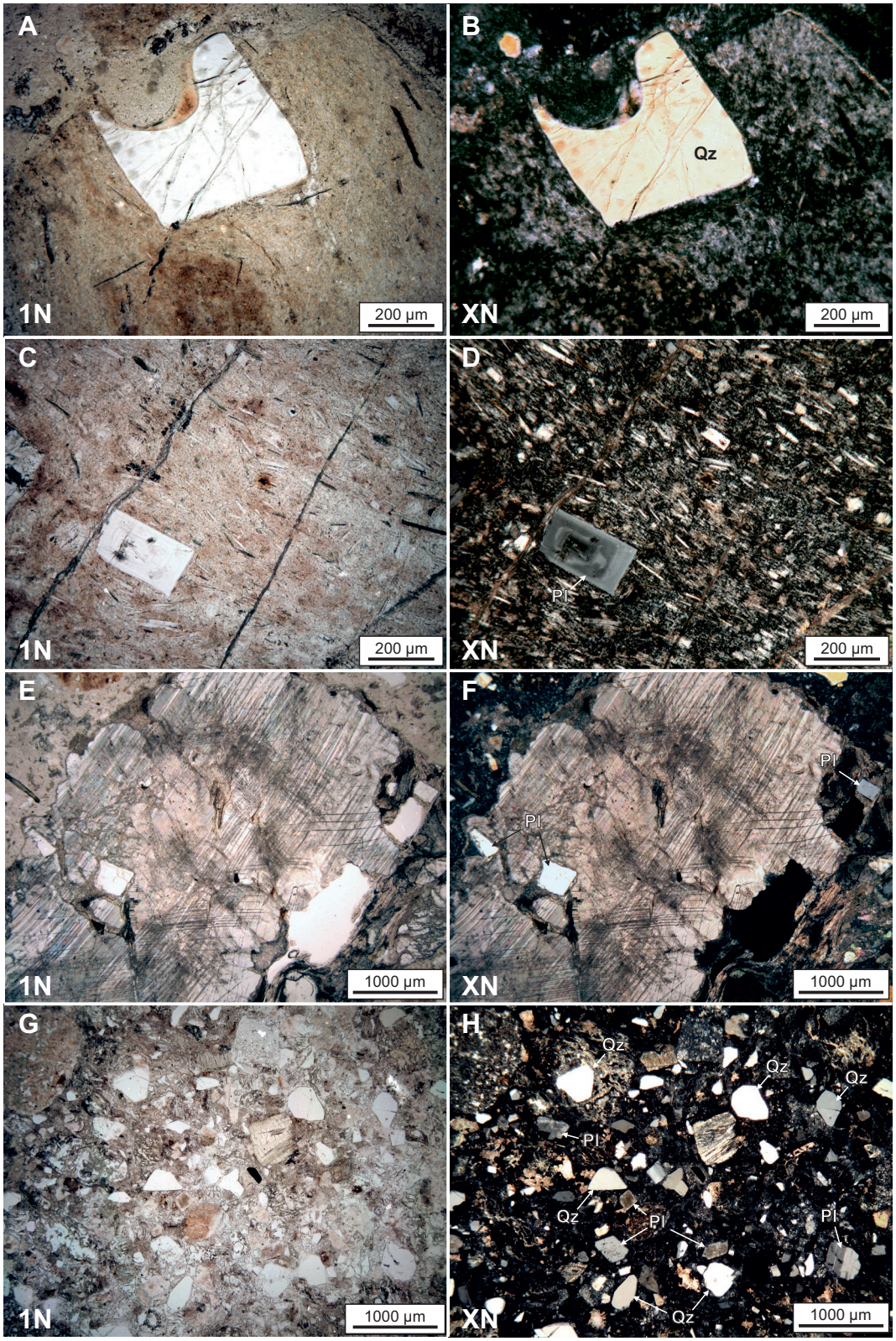

Fig. 3. Optical microscope images of the volcaniclastic matrix (**A–F**) and the rhyolitic clast (**G–H**). **A, B** — Embayed quartz phenocryst in the very fine-grained clay groundmass. **C, D** — Phenocryst of the euhedral, zoned plagioclase in the groundmass of the parallelly-oriented, fine-grained elongated plagioclase crystals. **E, F** — Carbonates with enclosed plagioclase crystals. **G, H** — Phenocrysts of quartz and plagioclase in very fine-grained, altered groundmass.

are also present. The macroscopic observations as well as observations carried with the optical microscope reveal a chaotic structure of the matrix and hyaline aphyric to slightly porphyritic texture marked by plagioclase, quartz, amphibole and biotite crystals and micro-crystals (Fig. 3A–D).

The volcanic breccia consists of subhedral phenocrysts of plagioclase, K-feldspar and quartz that commonly preserve crystal faces or embayments indicating volcanic source (Fig. 3A–B). The feldspars are partially to completely altered via sericitization. Rare biotite flakes are partially chloritized. Some clasts contain oscillatory zoned plagioclase crystals in groundmass composed of parallelly-oriented elongated plagioclase laths (Fig. 3C–D). Large, subangular clasts composed of carbonates occasionally enclose subhedral feldspars or quartz (Fig. 3E–F). The phenocrysts and clasts are dispersed in a very fine-grained matrix of minerals too fine to identify.

Monazite composition and U–Th–total Pb dating

The monazite in the volcanic breccia matrix (RU04B/06/11) and the rhyolitic clast (RU04C/06/11) forms from euhedral crystals with well-preserved crystal faces to anhedral crystals sizing from ca. 10 to 65 µm. The textural position of monazite in both investigated samples is in the fine-grained matrix of the rock. The monazite show faint patchy zoning (Fig. 4G–I),

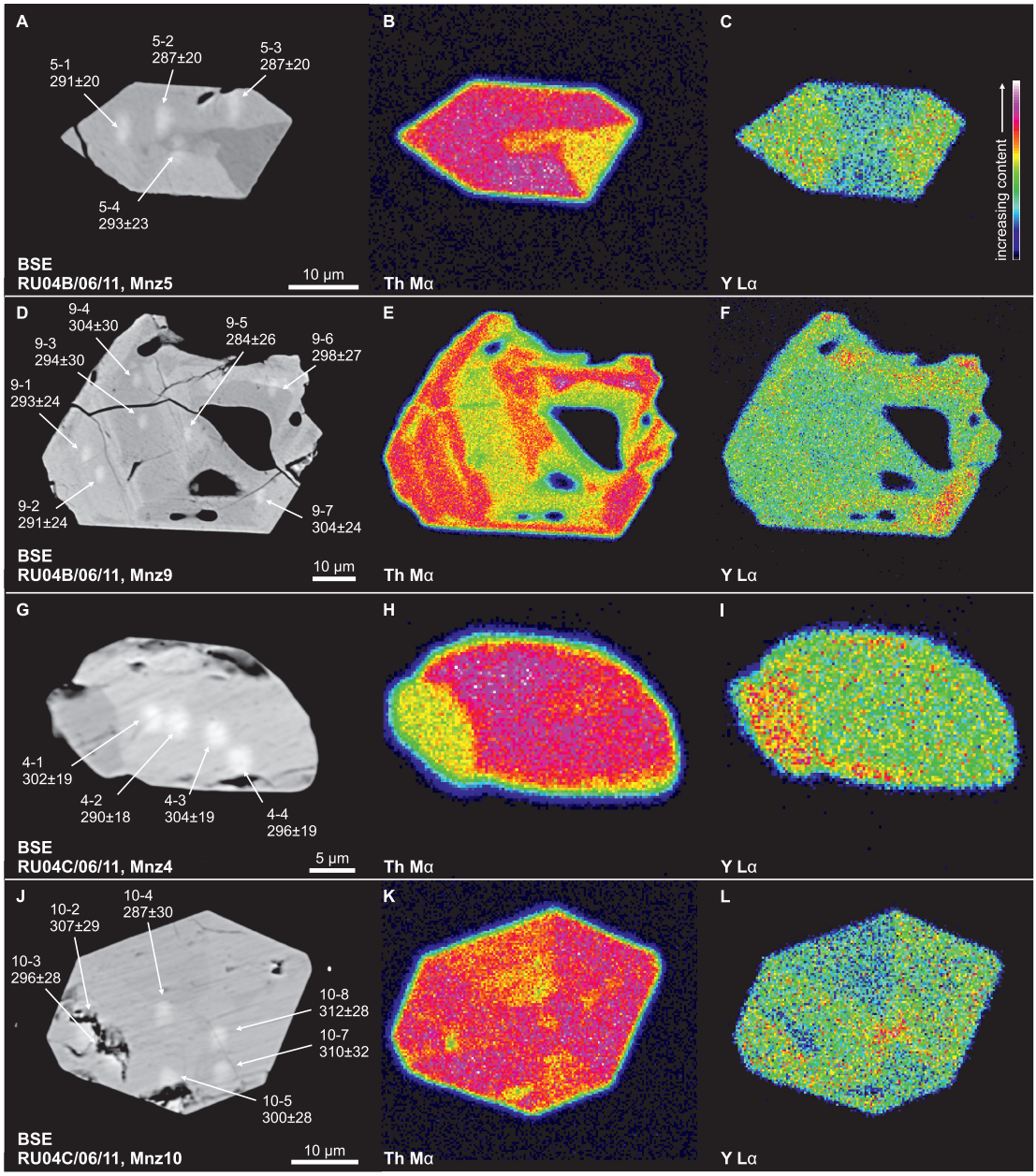

Fig. 4. Representative BSE images and compositional WDS X-ray maps of Th and Y of investigated monazite crystals. Analysis labels correspond to data in Table 1; ages (Ma) are given with 2σ error.

oscillatory growth zoning (Fig. 4D–F) or sector zoning (Fig. 4A–C, J–L). The monazite has high concentrations of Th (8.87–17.59 wt. % ThO_2 in RU04B/06/11; 8.79–18.23 wt. % ThO_2 in RU04C/06/11), low concentrations of U (0.15–0.54 wt. % UO_2 in RU04B/06/11; 0.20–0.57 wt. % UO_2 in RU04C/06/11), and slightly elevated concentrations of Y (0.94–1.97 wt. % Y_2O_3 in RU04B/06/11; 0.83–2.13 wt. % Y_2O_3 in RU04C/06/11) (Table 1). The actinides content is mainly controlled by substitution of huttonite component in the monazite structure (Fig. 5B,D). Despite compositional variations (Table 1), which are mostly related to the exchange of REEs and actinides substitution, the chondrite-normalized Th+U+Y+REE distribution patterns of investigated monazite in both samples are similar (Fig. 5A,C) indicating origin related to the same source. A distinct negative anomaly of Eu is characteristic for a monazite crystallization preceded or accompanied by the crystallization of feldspars, which preferentially incorporate Eu in the structure. All features of the investigated monazites, particularly oscillatory and sector zoning indicating rapid growth, and high Th concentrations suggesting crystallization under high temperature conditions are indicative for the volcanic origin of monazite.

29 analyses of 9 monazite crystals in the matrix RU04B/06/11 yielded dates from 284 to 316 Ma providing a mean age of 297±4.8 Ma (2σ; Fig. 6A; Table 2). In the rhyolitic clast (RU04C/06/11), 28 analyses of 7 monazite crystals provided dates from 270 to 312 Ma with a mean age of 295±4.4 Ma (2σ; Fig. 6D; Table 2). Combined U–Th–total Pb data for the matrix and the rhyolitic clast provide the mean age of 296±3.2 Ma (2σ; Fig. 6G; Table 2).

Discussion

The monazite age data presented here for the first time from the Sirinia Valley are typical for the Early Permian volcanic activity not only in the South Carpathians, but also in various parts of the Late Paleozoic terranes. The Lower Permian volcanic rocks in the South Carpathians area are known from both Danubian Units; in the Romanian segment of the Upper Danubian and in its south-eastern prolongation, namely the Stara Planina area, as well as in the Serbian part of the Lower Danubian, namely the Vrška Čuka–Kutlov areas (see Vozárová et al. 2009, their fig. 5). The acidic, rhyolitic volcanic and volcaniclastic material prevail in the Romanian Danubian Units, whereas trachytic rocks occur mainly southwards, in Serbia (Seghedi et al. 2001). On the basis of the geochemical data, an intraplate setting for these rocks is suggested as related to linear access along a sub-parallel dyke system in an extensional setting of a rhyolitic magma, a consequence of post-Variscan extensional tectonics (Seghedi 2011). The Stephanian–Early Permian displacement induced the development of numerous small and isolated sedimentary basins with their independent drainage systems. The formation of the basins was associated with differentiated local tectonic subsidence, which induced the genesis of horsts and

Table 1: Representative results of the EPMA compositional measurements of the investigated monazites (in wt. %).

Analysis	P_2O_5	As_2O_5	SiO_2	ThO_2	UO_2	Y_2O_3	La_2O_3	Ce_2O_3	Pr_2O_3	Nd_2O_3	Sm_2O_3	Eu_2O_3	Gd_2O_3	Tb_2O_3	Dy_2O_3	Ho_2O_3	Er_2O_3	Tm_2O_3	Yb_2O_3	Lu_2O_3	CaO	FeO	SrO	PbO	SO_3	Total
RU04B/06/11																										
3-1	24.71	0.15	2.20	11.86	0.24	0.96	14.12	26.77	2.89	9.81	1.54	<0.07	0.99	<0.08	0.30	<0.08	0.31	0.06	0.14	0.10	0.85	0.25	<0.03	0.16	0.03	98.44
5-2	23.17	0.14	3.65	17.54	0.44	1.39	12.23	23.55	2.67	9.72	1.78	<0.07	1.19	0.12	0.41	<0.08	0.39	0.12	0.16	<0.08	0.89	<0.04	<0.03	0.23	0.03	99.80
7-4	25.89	0.14	1.42	8.87	0.15	1.01	14.51	27.83	3.01	10.52	1.67	<0.07	0.91	0.09	0.29	<0.08	0.36	0.07	0.12	0.10	0.74	<0.04	<0.03	0.12	0.01	97.83
7-5	25.87	0.13	1.42	9.00	0.18	0.97	14.79	27.91	2.93	10.29	1.62	0.08	0.94	0.09	0.30	<0.08	0.30	0.08	0.10	0.10	0.74	<0.04	<0.03	0.12	0.01	97.98
9-1	24.28	0.13	2.60	14.38	0.34	1.48	11.94	24.23	2.86	10.52	2.14	<0.07	1.46	0.13	0.50	<0.08	0.38	0.09	0.11	0.10	0.81	0.10	<0.03	0.19	0.02	98.80
9-6	24.64	0.13	2.08	12.23	0.34	1.67	12.49	25.25	2.96	11.02	2.15	<0.07	1.43	0.15	0.51	<0.08	0.43	0.07	0.14	0.10	0.82	<0.04	<0.03	0.17	0.02	98.79
11-4	24.66	0.13	2.65	15.97	0.53	1.97	11.15	23.18	2.70	10.42	2.08	<0.07	1.55	0.11	0.60	<0.08	0.40	0.08	0.15	0.11	1.12	0.85	<0.03	0.22	0.06	100.69
RU04C/06/11																										
2-2	26.09	0.23	2.00	9.85	0.23	0.84	14.73	27.43	2.86	9.93	1.51	0.07	0.98	0.14	0.25	<0.08	0.34	0.07	0.12	0.09	0.88	<0.04	<0.03	0.13	0.03	98.77
3-1	27.01	0.24	1.55	8.79	0.21	1.09	14.23	27.71	3.07	10.93	1.72	<0.07	1.24	0.09	0.36	<0.08	0.39	0.07	0.16	0.10	0.80	<0.04	<0.03	0.12	0.02	99.90
4-2	23.76	0.23	3.66	17.94	0.54	1.52	11.11	22.99	2.66	9.79	2.05	<0.07	1.56	0.14	0.53	<0.08	0.39	0.09	0.14	0.10	0.88	<0.04	<0.03	0.24	0.02	100.33
4-3	23.64	0.21	3.72	17.65	0.52	1.51	11.09	22.81	2.66	10.02	2.00	<0.07	1.48	0.08	0.45	<0.08	0.39	0.11	0.18	<0.08	0.91	<0.04	<0.03	0.25	0.02	99.71
4-4	23.98	0.23	3.73	17.48	0.55	1.58	10.98	22.80	2.75	9.93	2.04	<0.07	1.48	0.14	0.48	<0.08	0.40	0.09	0.15	0.12	0.92	<0.04	<0.03	0.24	0.03	100.13
9-4	24.34	0.24	2.90	15.86	0.57	2.13	10.65	22.65	2.76	10.46	2.20	<0.07	1.63	0.11	0.61	<0.08	0.42	0.12	0.15	0.10	1.04	<0.04	<0.03	0.22	0.02	99.18
9-6	24.45	0.25	2.83	16.03	0.53	2.05	10.65	22.63	2.70	10.39	2.20	<0.07	1.68	0.15	0.63	<0.08	0.49	0.10	0.14	<0.08	1.04	<0.04	<0.03	0.22	0.02	99.17
10-5	26.02	0.28	1.88	11.05	0.24	1.07	13.48	26.62	2.90	10.63	1.70	<0.07	1.18	0.11	0.35	<0.08	0.35	0.08	0.17	0.10	0.84	<0.04	<0.03	0.15	0.02	99.24

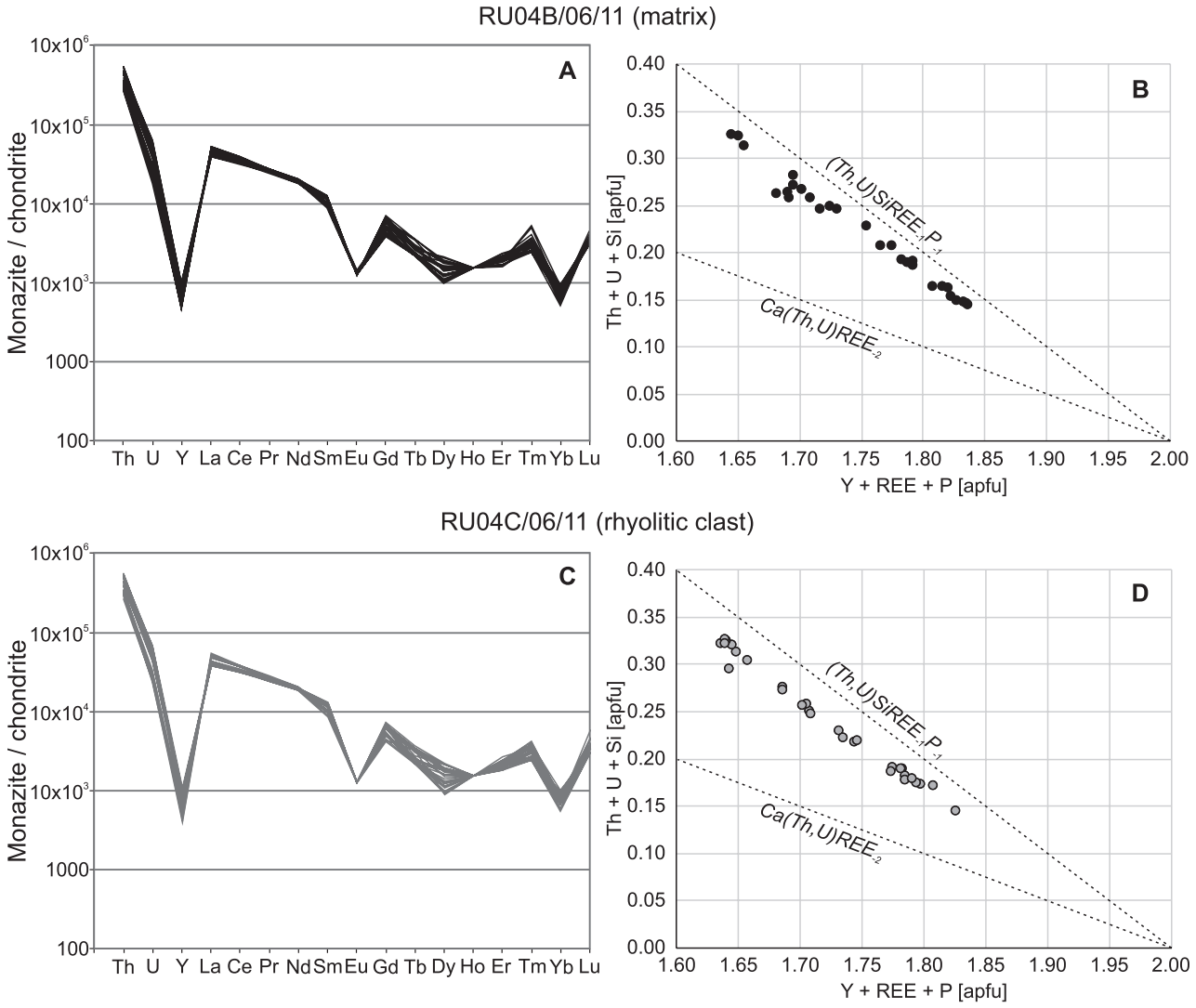

Fig. 5. A, C — Chondrite-normalized Th+U+Y+REE distribution patterns of investigated monazites. CI chondrite composition after McDonough and Sun (1995). **B, D —** Plots of formula proportions of (Y+REE+P) vs. (Th+U+Si) calculated on the basis of 4 oxygen atoms for the investigated monazites in the matrix of volcanic breccia RU4B/06/11 and the rhyolitic clast RU04C/06/11. Dashed lines represent the huttonitic substitution of (Th, U)SiREE$_{-1}$P$_{-1}$ and cheralitic substitution of Ca(Th, U)REE$_{-2}$ (cf., Förster 1998; Linthout 2007).

grabens as well as of magmatic activity. In many occurrences, the lavas are interbedded with sediments indicating a coeval extension and subsidence with magmatic activity across Central Europe (Vozárová et al. 2009). The U–Pb and Ar–Ar dating of plutonic and volcanic rocks constrained 305–290 Ma period of the magmatic activity (Timmerman 2008), which is concordant with the monazite ages obtained from the South Carpathians (this study). The post-Variscan sequence of the South Carpathians has been separated in two basins, possibly isolated by emerged ridges (fig. 3 in Kräutner 1996). The Upper Danubian Unit, where the volcaniclastics were sampled, include two sub-basins (Presacina sedimentary zone in the East and Sirinia sedimentary zone in the West) separated by a small emerged Iablanita-Rudaria crystalline zone (Năstăseanu et al. 1981; Berza et al. 1994).

The previous studies indicate that the volcanic activity in the South Carpathian area began during the Early Cisuralian, after the sedimentation period of clastic and locally fresh-water limestones (Seghedi et al. 2001; Seghedi 2011).

The monazite age of 296±3.2 Ma (Asselian) for the volcaniclastic matrix and the rhyolite clasts of the Sirinia Basin is slightly older than the previously suggested volcanic interval of ca. 280–290 Ma (Seghedi et al. 2001; Vozárová et al. 2009). However, the previous studies did not constrain the isotopic age of the beginning of rhyolitic activity. Recent studies of the Permian succession from the Sirinia Basin, reported the occurrence of exclusive rhyolitic clasts in the conglomerates that occur close (about 7 km southward) to our sampling site, and the simultaneous decline of their content of the rhyolitic clasts westward (Nuțu-Dragomir 2017).

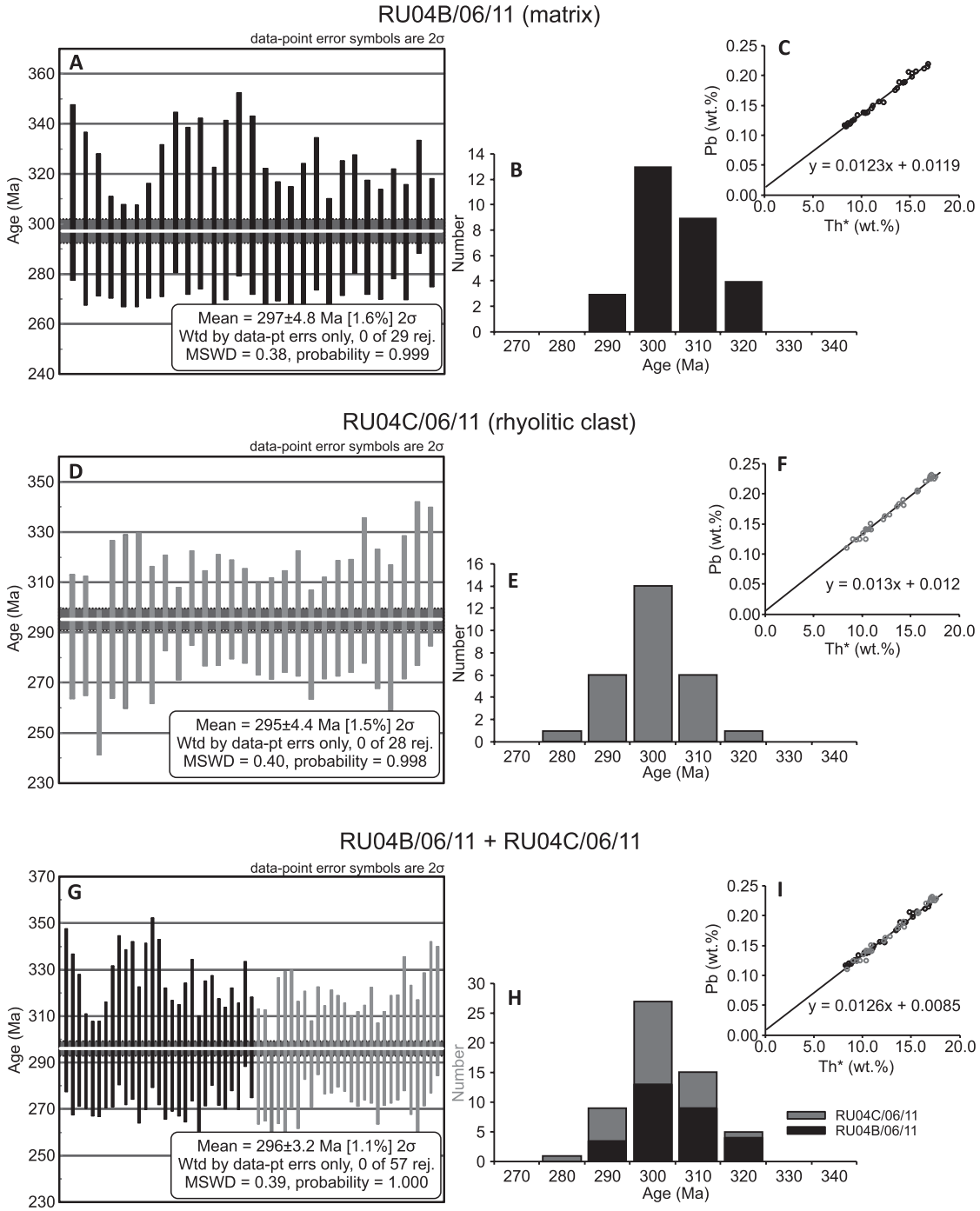

Fig. 6. Results of the U–Th–total Pb dating of monazite in (**A–C**) the matrix of volcanic breccia RU4B/06/11; and (**D–F**) the rhyolitic clast RU04C/06/11. **G–I** — Combined monazite data from matrix of volcanic breccia and the rhyolitic clast interpreted as single age population.

The explanation of the differentiated clast composition from the conglomerates described by Nuțu-Dragomir (2017) is difficult due to the lack of trustworthy correlative horizons. Therefore, they may represent various parts of the lower Permian succession.

According to Heckel and Clayton (2006), the Lower Autunian refers to the terminal Gzhelian and therefore the Sirinia Valley volcaniclastics can be interpreted as Carboniferous as well. Vozárová et al. (2009) and Seghedi (2011) used the standard Permian subdivisions and according to them, the older Permian volcanic rocks in the basin are Cisuralian in age and the sequence containing volcaniclastics is separated by a narrow stratigraphic gap ranging in age from Upper Moscovian to Kasimovian or even Gzhelian.

The monazite data obtained for the volcaniclastic rocks of the Trescovăț Formation indicate the Asselian age (basal Cisuralian). This suggests that the effusive stage of the volcanic activity started during the Early Permian, close to

Table 2: Results of the monazite dating presenting also Th, U, Pb, Y and calculated Th* values. Th* values are calculated according to Konečný et al. (2018).

Analysis	Th	±2σ	U	±2σ	Pb	±2σ	Y	Th*	Age (Ma)	±2σ
RU04B/06/11										
2-1	7.950	0.071	0.204	0.012	0.120	0.006	0.923	8.61	313	35.1
2-2	8.125	0.073	0.208	0.012	0.119	0.006	0.973	8.80	302	34.6
3-1	10.422	0.090	0.228	0.013	0.149	0.006	0.758	11.16	300	28.3
5-1	15.459	0.127	0.432	0.014	0.219	0.006	1.244	16.86	291	20.3
5-2	15.413	0.127	0.414	0.014	0.215	0.006	1.097	16.75	287	20.4
5-3	15.175	0.125	0.395	0.014	0.211	0.006	0.922	16.46	287	20.3
5-4	13.312	0.111	0.335	0.013	0.189	0.006	0.986	14.40	293	22.8
6-1	9.605	0.084	0.202	0.012	0.138	0.006	0.741	10.26	301	30.3
6-2	8.976	0.079	0.190	0.012	0.134	0.006	0.860	9.59	313	32.1
6-3	8.619	0.076	0.198	0.012	0.126	0.006	0.912	9.26	305	33.3
7-1	8.430	0.075	0.174	0.012	0.124	0.006	0.753	8.99	308	34.0
7-2	9.883	0.086	0.221	0.012	0.139	0.006	0.821	10.60	293	29.3
7-3	7.869	0.070	0.169	0.012	0.115	0.006	0.771	8.42	306	35.7
7-4	7.797	0.070	0.150	0.012	0.117	0.006	0.792	8.28	316	36.4
7-5	7.912	0.071	0.170	0.012	0.116	0.006	0.760	8.46	308	35.6
8-2	10.270	0.088	0.241	0.013	0.145	0.006	0.871	11.05	294	28.2
9-1	12.635	0.106	0.326	0.013	0.179	0.006	1.167	13.69	293	23.8
9-2	12.384	0.104	0.340	0.013	0.175	0.006	1.189	13.48	291	23.9
9-3	9.620	0.084	0.245	0.013	0.137	0.006	1.086	10.42	294	29.7
9-4	9.411	0.082	0.247	0.013	0.139	0.006	1.074	10.21	304	30.4
9-5	11.308	0.096	0.296	0.013	0.156	0.006	1.102	12.27	284	25.7
9-6	10.750	0.092	0.317	0.013	0.157	0.006	1.313	11.78	298	26.9
9-7	12.610	0.106	0.397	0.013	0.189	0.006	1.479	13.90	304	23.6
10-2	13.049	0.109	0.386	0.013	0.188	0.006	1.108	14.30	295	22.9
10-3	13.741	0.115	0.437	0.013	0.198	0.006	1.385	15.16	292	21.9
11-1	13.701	0.114	0.452	0.014	0.203	0.006	1.541	15.17	300	22.0
11-2	12.853	0.108	0.486	0.014	0.189	0.006	1.474	14.43	293	22.9
11-3	13.172	0.110	0.504	0.014	0.206	0.006	1.534	14.81	311	22.6
11-4	14.034	0.117	0.490	0.014	0.207	0.006	1.552	15.62	297	21.6

the Carboniferous/Permian boundary. Three different rock types have been assigned to the subaqueous effusive phase at this stage (Seghedi 2011): (i) lava domes and flows closely associated with (ii) primary volcaniclastic deposits formed during shattering and quenching of lava domes, and (iii) secondary stratified deposits resulting from transformation of the volcaniclastic deposits into subaqueous gravity flows.

Despite the robust age dataset with a tight cluster of U–Th–total Pb dates, the precision of electron microprobe analysis is not sufficient to distinguish two events with a gap of only several million years between them. Consequently, monazite data in both samples with mean ages within error (297±4.8 Ma and 295±4.4 Ma), are considered as representing a single age population of 296±3.2 Ma, which indicates timing of monazite crystallization in the magma chamber prior to extrusion. Nevertheless, it cannot be excluded that the data demonstrate a record of two or more overlapping monazite age populations and therefore at least two separate magmatic events, which are indistinguishable due to analytical limitations.

The origin of the breccia can be related to a subaqueous–subaerial explosive phase and to a deposition from the column collapse of tephra jets as pyroclastic debris flow (Seghedi 2011). The previously deposited volcaniclastics, which were covered by domes composed of massive rhyolites, have been activated due to the erosion inducing unstable slope of the domes and to the subsequent turbulent high viscosity flow that mixed up rhyolitic clasts with their volcaniclastic matrix. The variation of such a scenario assumes the explosive genesis of the volcaniclastic breccia. In this idea, the folding and breaking of the dome shell allowed a new supply of magma to arrive in contact with water and to erupt explosively (Seghedi 2011). During the eruption, the previously accumulated material could be moved together with freshly thrown rhyolitic fragments and they were later deposited or even resedimented as debris flows or lahars. Due to small exposures and to the tectonic deformations of the area, it is difficult to identify the most probable scenario. The reconstruction assumes a short time gap between the crystallization of the investigated monazites and further deposition of the volcaniclastic breccia. Since the magmatic activity related to rhyolitic volcanism is usually characterized by a short lifespan ranging from <4 years to ca. 100 ka (cf. Carrasco-Núñez & Riggs 2008, and references therein), the timespan from monazite crystallization and eruption to deposition of the investigated volcaniclastic rocks is significantly shorter that the 3.2 Ma 2σ error of the monazite mean age. Consequently, the 296±3.2 Ma age is proposed as the maximum depositional age for the investigated volcaniclastic rocks.

Conclusions

The investigated volcaniclastic rocks from the Sirinia Basin of the Upper Danubian Nappe contain rhyolitic clasts with size indicative for short transportation, probably related to high viscosity debris flow from local sub-aqueous effusive rhyolites.

The monazite age of 296±3.2 Ma constraints timing of the volcanic activity to the early Permian (Asselian–lowermost Cisuralian) and is proposed as the maximum depositional age of the volcaniclastic rocks in the Sirinia Basin.

Acknowledgements: Patrik Konečný and Gabriela Kozub-Budzyń are greatly acknowledged for their assistance with electron microprobe analyses. This work was partially funded by the ING PAN Research Funds (Projects "REE" and "DEMISS"). The authors thank Ioan Seghedi, two anonymous reviewers and handling Editor Igor Petrík for their

useful comments, which strongly influenced the final shape of the manuscript.

References

Berza T., Krautner H.G. & Dimitrescu R. 1983: Nappe structure of the Danubian window of the Central South Carpathians. *An. Inst. Geol. Geof.* 60, 31–39.

Berza T., Iancu V., Seghedi A., Nicolae I., Balintoni I., Ciulavu D. & Bertotti G. 1994: ALCAPA II. Excursion to South Carpathians, Apuseni Mountains and Transylvania Basin: Description of stops. *Rom. J. Tect. Reg. Geol*. 75, 2, 105–149.

Carrasco-Núñez G. & Riggs N.R. 2008: Polygenetic nature of a rhyolitic dome and implications for hazard assessment: Cerro Pizarro volcano, Mexico. *J. Volcano. Geotherm. Res*. 171, 307–315. https://doi.org/10.1016/j.jvolgeores.2007.12.002

Codarcea A. 1940: Vues nouvelles sur la tectonique du Banat meridional et du Plateau de Mehedinţi. *D. S. Inst. Geol. Rom*. 20, 1–74.

Codarcea A., Răileanu G., Pavelescu L., Gherasi N., Năstăseanu S., Bercia I. & Mercus D. 1961: General view on the geological structure of the South Carpathians between the Danube and Olt. CBGA Congress V, *Excursion Guide C. South Carpathians*, Bucureşti, 1–126.

Dragastan O., Popa M.E. & Ciupercianu M. 1997: The Late Palaeozoic phytostratigraphy and palaeoecology of the South Carpathians (Romania). In: Primul Simpozion Naţional de Paleontologie. Bucureşti, 57–64.

Förster H.-J. 1998: The chemical composition of REE–Y–Th–U-rich accessory minerals in peraluminous granites of the Erzgebirge-Fichtelgebirge region, Germany, Part I: The monazite-(Ce)-brabantite solid solution series. *Am. Mineral.* 83, 259–272. https://doi.org/10.2138/am-1998-3-409

Heckel P.H. & Clayton G. 2006: The Carboniferous System. Use of the new official names for the subsystems, series, and stages. *Geol. Acta.* 4, 403–407. https://doi.org/10.1344/105.000000354

Konečný P. Kusiak M.A. & Dunkley D.J. 2018: Improving U–Th–Pb electron microprobe dating using monazite age references. *Chem. Geol.* 484, 22–35. https://doi.org/10.1016/j.chemgeo.2018.02.014

Linthout K. 2007: Tripartite division of the system $2REEPO_4$–$CaTh(PO_4)_2$–$2ThSiO_4$, discreditation of brabantite, and recognition of cheralite as the name for members dominated by $CaTh(PO_4)_2$. *Can. Mineral.* 45, 503–508. https://doi.org/10.2113/gscanmin.45.3.503

Ludwig K.R. 2012: Isoplot 3.75. A geochronological toolkit for Microsoft Excel. *Berkeley Geochronology Center Special Publication* 5, 1–75.

McDonough W.F. & Sun S.-s. 1995: The composition of the Earth. *Chem. Geol.* 120, 223–253. https://doi.org/10.1016/0009-2541(94)00140-4

Montel J.M., Foret S., Veschambre M., Nicollet C. & Provost A. 1996: Electron microprobe dating of monazite. *Chem. Geol.* 131, 37–53.

Munteanu-Murgoci G. 1905: Sur l'existence d'une grande nappe de recouvrement dans les Carpathes meridionales. *C. R. Acad. Sci.* 4, 337–339.

Năstăseanu S., Stănoiu I. & Bițoianu C. 1973: Correlation of Hercynian (Westphalian–Permian) molasse formations from the Western part of the South. *A. Inst. Geol*. XL, 71-109 (in Romanian).

Năstăseanu S., Bercia I., Iancu V., Vlad Ş. & Hârtopanu I. 1981: The structure of the South Carpathians (Mehedinţi – Banat Area). *Guide to excursion B 2. Carp. Balk. Geol. Assoc. XIIth Congr*. Bucharest, *IGR*, 1–100.

Nuțu-Dragomir M-L. 2017: Sedimentary characteristics of a Permian continental succession in Sirinia Basin (South Carpathians, Romania). In: Anon (Ed.): Conference Proceedings, 17th International Multidisciplinary Scientific GeoConferences SGEM, 29.06-05.07-05.2017, Albena, Bulgaria. *STEF92Technology Ltd.* Sofia, Bulgaria, 503–514.

Petrescu I., Nicorici E., Bițoianu C., Țicleanu N., Todros C., Ionescu M., Mărgărit G., Nicorici M., Duşa A., Pătruțoiu I., Munteanu A. & Buda A. 1987: Coal geology. Vol. 2., *Editura Tehnică*, Bucharest, 1–385 (in Romanian).

Pop G., Mărunţiu M., Iancu V., Seghedi A. & Berza T. 1997: Geology of the South Carpathians in the Danube Gorges. *Field guidebook*, *Inst. Geol. Rom.*, Bucharest, 1–28.

Popa M.E. 2005: Aspects of Romanian Palaeozoic Palaeobotany and Palynology. Part II. Overview of the Upper Carboniferous formations in the South Carpathians. *Z. Dtsch. Ges. Geol*. 156, 415–430. https://doi.org/10.1127/1860-1804/2005/0156-0415

Popa M.E. & Anastasiu N. 2019: Coal resources. In: Constantinescu E. & Anastasiu N. (Eds.): Mineral resources of Romania. Vol. III. Energy resources. *Romanian Academy Press*, Bucureşti, 435-504 (in Romanian).

Popa M.E. & Cleal C.J. 2012: Aspects of Romanian Palaeozoic P alaeobotany and Palynology. Part III. The Late Carboniferous flora of Baia Nouă, Sirinia Basin. *Geol. Croat*. 65, 329–243. https://doi.org/10.4154/GC.2012.22

Preda I., Turculeţ I., Bădăluţă A., Barus T. & Androhovici A. 1994. Coal Geology. Part II. Occurrence of coal. *Editura Universităţii din Bucureşti,* Bucureşti, (in Romanian).

Răileanu G. 1953: Geological researches in the Sviniţa–Faţa Mare region. *Bul. Ştiinţific, Secţ. Ştiinţe Biol. Agro. Geol. Geogr.* 5, 307–409 (in Romanian).

Răileanu G. 1960: Recherches geologiques dans la region Sviniţa-Faţa Mare. *Ann. Com. Geol*. XXVI–XXVIII, 347–383.

Răileanu G., Grigoraş N., Oncescu N. & Plişcă T. 1963: Coal Geology with special emphasis on the Romanian territory. *Editura Tehnică*, Bucureşti, 1–344 (in Romanian).

Seghedi I. 2011: Permian rhyolitic volcanism, changing from subaqueous to subaerial in post-Variscan intra-continental Sirinia Basin (SW Romania–Eastern Europe). *J. Volc. Geotherm. Res.* 201, 312–324. https://doi.org/10.1016/j.jvolgeores.2010.07.015

Seghedi A., Popa M., Oaie G. & Nicolae I. 2001: The Permian system in Romania. *Natura Bresciana, Ann.Mus.Civ.Nat.*, Brescia, 25, 281–293.

Stan N., Colios E. & Bratosin, I. 1986: Permian ignimbritic rocks of the South Banat (Sviniţa–Baia Nouă–Tâlva Frasinului). *D.S. Inst. Geol. Geofiz*. 70–71, 203–216.

Stănoiu I. & Stan N. 1986: Lithostratigraphy of the Permian–Carboniferous molasse in the Munteana–Sviniţa–Tâlva Frasinului region (South Banat). *Dări de Seamă Inst. Geol. Geof.* 70–71, 39–50 (in Romanian).

Streckeisen A. 1934: Sur la tectonique de Carpathes Meridionales. *An. Inst. Geol*. 16, 327–481.

Timmerman M.J. 2008: Palaeozoic magmatism. In: McCann T. (Ed.): The Geology of Central Europe, Precambrian and Palaeozoic, vol. 1. *Geological Society*, London, 665–748.

Vozárová A., Ebner F., Kovács S., Kräutner H.-G., Szederkenyi T., Krstić B., Sremac J., Aljinovič D., Novak M. & Skaberne D. 2009: Late Variscan (Carboniferous to Permian) environments in the Circum Pannonian Region. *Geol. Carpath.* 60, 71–104. https://doi.org/10.2478/v10096-009-0002-7